

Finite Element Analysis of Permanent Magnet Synchronous Generator

A Thesis Submitted in Partial Fulfilment of the
requirements for the Degree of
MASTER OF ELECTRICAL ENGINEERING, 2016

By

SOUMYAJIT CHOWDHURY

(Roll No. 001410802006)

Exam. Roll No. M4ELE1605

Reg No. 128893 of 14-15

Under the Supervision of

DR. MADHAB ROY

**DEPARTMENT OF ELECTRICAL ENGINEERING
FACULTY OF ENGINEERING AND TECHNOLOGY**

JADAVPUR UNIVERSITY

188, Raja S.C. Mallick Road, Kolkata-700032

CERTIFICATE

This is to certify that this dissertation entitled “**Finite Element Analysis of Permanent Magnet Synchronous Generator**” has been carried out by **SOUMYAJIT CHOWDURY** under my guidance and supervision and be accepted in partial fulfilment of the requirement for the degree of **Master of Electrical Engineering**. The project, in my opinion, is worthy of its acceptance.

SUPERVISOR

Dr. Madhab Roy

Associate Professor
Department of Electrical Engineering
Jadavpur University

Countersigned by

**Prof. (Dr.) Swapan Kumar
Goswami**

Head of the Department
Electrical Engineering Department
Jadavpur University

Prof. Sivaji Bandyopadhyay

Dean of the Faculty of
Engineering and Technology
Jadavpur University

CERTIFICATE OF APPROVAL*

The foregoing thesis is hereby approved as a creditable study of an engineering subject and presented in a manner satisfactory to warrant acceptance as pre-requisite to the degree for which it has been submitted. It is understood that by this approval the undersigned do not necessarily endorse or approve any statement made, opinion expressed or conclusion drawn there in but approve the thesis for which it is submitted.

Committee on final Examination for
Evaluation of the thesis

(Signature of the Examiners)

* Only in case Thesis is approved.

Declaration

I certify that except where due to acknowledgement has been made; the work is that of the candidate alone. This thesis is a presentation of my original research work and has not been submitted previously, in whole or in part, to qualify for any other academic award. Furthermore, the content of the thesis is the result of work which has been carried out since the official commencement date of the approved research program.

The work was done under the guidance of Professor Dr. Madhab Roy, Jadavpur University, Kolkata.

Name : Soumyajit Chowdhury

Roll No. : M4ELE1605

Thesis Title : Finite Element Analysis of
Permanent Magnet Synchronous
Generator.

Signature :

Date :

ACKNOWLEDGEMENT

I take this opportunity to express my profound gratitude and deep regards to my guide *Prof. (Dr.) Madhab Roy* for their exemplary guidance, monitoring and constant encouragement throughout the course of this thesis. The blessing, help and guidance given by them time to time will carry me a long way in the journey of life on which I am about to embark. I thank my fellow classmates and all PhD scholars of machine and drives lab, for the simulating discussion, for the sleepless nights we were working together before deadlines, and for all the fun we have had in the last two years.

I would like to thank *Prof. (Dr.) Swapan Kumar Goswami*, Head of the Department, Electrical Engineering, for providing me with the necessary facilities for carrying out this thesis.

Last but not the least, I would like to express my deep thanks to my family for their unlimited support and encouragements. Their prayer and love was my source and motivation to continue and finish this research.

TABLE OF CONTENTS

<u>CHAPTER</u>	<u>PAGE</u>
Introduction-----	-----(i)
Literature Review-----	-----(iv)
1. Principal Laws and Methods in Electrical Machine Design---	-----1
1.1 Electromagnetic principles-----	-----1
1.2 Numerical Solution-----	-----9
2. The Finite Element Method-----	----15
2.1 Finite Element Discretization-----	----15
2.2 Element Governing Equations-----	----17
2.3 Assembling of All Elements-----	----22
2.4 Solving the Resulting Equations-----	----25
3. Permanent Magnet Materials -----	----29
3.1 Demagnetization curve and magnetic parameters-----	----29
3.2 Early history of permanent magnets-----	----32
3.3 Properties of permanent magnets-----	----33
4. COMSOL Multiphysics Application-----	----38
4.1 Finite Element Method as an aid to Machine Design----	----38
4.2 Commercial Software-----	----38
4.3 COMSOL Multi Physics application-----	----40
Conclusion-----	-----(v)
References-----	-----(vi)

Introduction

This thesis provides an overview of the state of art in computational electromagnetic. There are three major areas like Design, optimization and material selection for the electric machines. The computational tool based on finite elements is very useful and powerful field simulation techniques available to assist in the design and performance prediction of electric machines. But the complexity in the geometry and multi material composition often hampers widespread use of these techniques. Commercial software, based on finite element Comsol Multi physics is very advanced and provides a reliable tool for 2D and 3D analysis in particular for multi-physics and optimization problems. The present work emphasized on the Recent advances in design and simulation software improving the standards of research and development.

Synchronous Generator

It converts mechanical energy to electrical energy in the form of alternating current. For reasons of cost and simplicity, most alternators use a rotating magnetic field with a stationary armature.

A conductor moving relative to a magnetic field develops an electromotive force (EMF) in it according to Faraday's Law of electromagnetic induction . This emf reverses its polarity when it moves under magnetic poles of opposite polarity. Typically, a rotating magnet, called the rotor turns within a stationary set of conductors wound in coils on an iron core, called the stator. The field cuts across the conductors, generating an induced EMF (electromotive force), as the

mechanical input causes the rotor to turn. The rotating magnetic field induces an AC voltage in the stator windings. Since the currents in the stator windings vary in step with the position of the rotor. The rotor's magnetic field may be produced by permanent magnets, or by a field coil electromagnet.

Permanent Magnet Synchronous Generator

The excitation field is provided by a permanent magnet instead of a coil. The term synchronous refers here to the fact that the rotor and magnetic field rotate with the same speed, because the magnetic field is generated through a shaft mounted permanent magnet mechanism and current is induced into the stationary armature. Permanent magnet machines avoid the loss due to magnetizing current in the rotor, but are restricted in size, due to the cost of the magnet material. Since the permanent magnet field is constant, the terminal voltage varies directly with the speed of the generator.

Synchronous generators are the majority source of commercial electrical energy. They are commonly used to convert the mechanical power output of steam turbines, gas turbines, reciprocating engines and hydro turbines into electrical power for the grid. Wind turbines of any significant scale use asynchronous generators exclusively.

Thesis Overview :-

In this Thesis Electromagnetic Principles of Electrical Machine Design and the Finite Element Analysis Method, a approach to machine design are discussed. The finite element analysis is used in Comsol environment. We have taken a 8 pole Permanent Magnet Synchronous Generator , Samarium Cobalt is used as the permanent magnet in rotor. Changing the Number of turns in Stator winding and RPM of the generator the change in induced voltage is observed.

- Chapter 1 :- the Electromagnetic Principles and laws of Electrical Machine Design is discussed.
- Chapter 2 :- overview of Finite element Method.
- Chapter 3 :- Permanent Magnet Materials, it's properties and application.
- Chapter 4 :- Comsol Multiphysics application.

LITERATURE REVIEW

- *Charanjiv Gupta, Sanjay Marwaha and Manpreet Singh Manna in "Finite Element method as an aid to Machine Design: A Computational Tool" , provides an overview of the state of art in computational electromagnetic. There are three major areas like Design, optimization and material selection for the electric machines. It gives a brief introduction to the most important Commercial software available for machine design.*
- *Juha Pyrhönen , Tapani Jokinen and Valéria Hrabovcová in "Design of Rotating Electrical Machines " , provides basic Electromagnetic principles in Electrical machine design and also few approach to numerical solution of electromagnetic equations.*
- *Yao Duan and Dan M. Ionel in " A Review of Recent Developments in Electrical Machine Design Optimization Methods With a Permanent Magnet Synchronous Motor Benchmark Study " , covers the significant developments of the last decade, including surrogate modelling of electrical machines and direct and stochastic search algorithms for both single- and multi-objective design optimization problems.*
- *J. R. Brauer, G. A. Zimmerlee, T. A. Bush, R. J. Sandel, R. D. Schultz in "3D Finite Element Analysis of Automotive Alternators under any Load" , covers The electromagnetic performance of an automotive alternator is calculated under an arbitrary electrical load on its stator winding.*
- *Rakesh Kumar Jha, Arvind S. Pande, Prof. Harpreet Singh in " Design and Analysis of Synchronous Alternator for Reduction in Harmonics and Temperature by Short Pitch Winding" , covers Design and analysis of synchronous alternator for different chording factor and find the pitch factors for optimum efficiency and got the expected results which is excepted by industry.*

1.

Principal Laws and Methods in Electrical Machine Design :-

1.1 Electromagnetic Principles

A comprehensive command of electromagnetic phenomena relies fundamentally on Maxwell's equations. The description of electromagnetic phenomena is relatively easy when compared with various other fields of physical sciences and technology, since all the field equations can be written as a single group of equations. The basic quantities involved in the phenomena are the following five vector quantities and one scalar quantity:

Electric field strength	E	[V/m]
Magnetic field strength	H	[A/m]
Electric flux density	D	[C/m ²]
Magnetic flux density	B	[V s/m ²], [T]
Current density	J	[A/m ²]
Electric charge density, $\frac{dQ}{dV}$	ρ	[C/m ³]

The presence of an electric and magnetic field can be analysed from the force exerted by the field on a charged object or a current-carrying conductor. This force can be calculated by the Lorentz force (Figure-), a force experienced by an infinitesimal charge dQ moving at a speed v . The force is given by the vector equation

$$dF = dQ(E + v \times B) = dQE + \frac{dQ}{dt} dl \times B = dQE + idl \times B \quad \dots 1.1$$

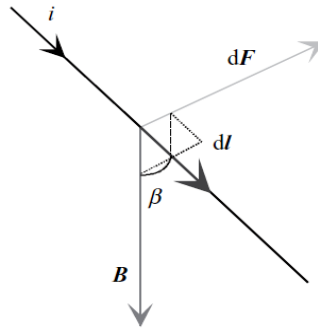


Figure : 1.1

dF --> Lorentz force acting

dl --> differential length of conductor

i --> electric current through conductor

B --> magnetic field flux density

β --> measured angle between the conductor and flux density vector B .

so, $idl \times B = idlB \sin \beta$.

In electrical engineering theory, the other laws, which were initially discovered empirically and then later introduced in writing, can be derived from the following fundamental laws presented in complete form by Maxwell. To be independent of the shape or position of the area under observation, these laws are presented as differential equations.

❖ Continuity equation of the electric current :-

A current flowing from an observation point reduces the charge of the point. This law of conservation of charge can be given as a divergence equation

$$\nabla \cdot J = -\frac{\partial \rho}{\partial t} \quad \dots 1.2$$

Maxwell's actual equations are written in differential form as

$$\nabla \times E = -\frac{\partial B}{\partial t} \quad \dots 1.3$$

$$\nabla \times H = J + \frac{\partial D}{\partial t} \quad \dots 1.4$$

$$\nabla \cdot D = \rho \quad \dots 1.5$$

$$\nabla \cdot B = 0 \quad \dots 1.6$$

❖ **Faraday's induction law (Equation 1.3) :-** This describes how a changing magnetic flux creates an electric field around it. Maxwell's equations often prove useful in their integral form: Faraday's induction law

$$\oint_l E \cdot dl = \frac{d}{dt} \int_s B \cdot dS = -\frac{d\phi}{dt} \quad \dots 1.7$$

states that the change of a magnetic flux Φ penetrating an open surface S is equal to a negative line integral of the electric field strength along the line l around the surface. Mathematically, an element of the surface S is expressed by a differential operator dS perpendicular to the surface. The contour line l of the surface is expressed by a differential vector dl parallel to the line.

Faraday's law together with Ampere's law are extremely important in electrical machine design. At its simplest, the equation can be employed to determine the voltages induced in the windings of an electrical machine. The equation is also necessary for instance in the determination of losses caused by eddy currents in a magnetic circuit, and when determining the skin effect in copper. Figure 1.2 illustrates Faraday's law. There is a flux Φ penetrating through a surface S , which is surrounded by the line l .

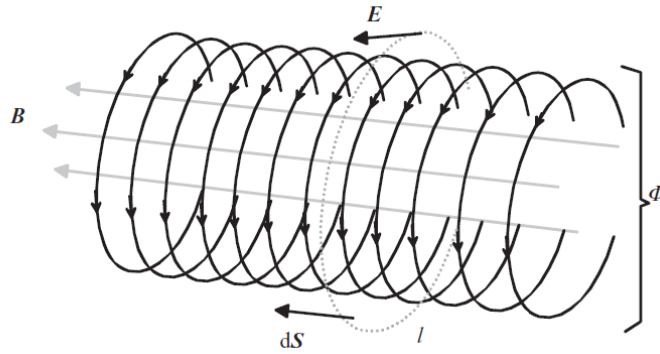


Figure : 1.2

dS --> a vector perpendicular to the surface S

l --> closed line to define the surface

Φ --> magnetic flux with a density B

E --> an electric current strength created by a change in flux density

The arrows in the circles point the direction of the electric field strength E in the case where the flux density B inside the observed area is increasing. If we place a short-circuited metal wire around the flux, we will obtain an integrated voltage $\oint E \cdot dl$ in the wire, and consequently also an electric current. This current creates its own flux that will oppose the flux penetrating through the coil.

If there are several turns N of winding (Figure 1.2), the flux does not link all these turns ideally, but with a ratio of less than unity. Hence we may denote the effective turns of winding by $k_w N$, ($k_w < 1$). Equation (1.7) yields a formulation with an electromotive force e of a multi-turn winding. In electrical machines, the factor k_w is known as the winding factor. This formulation is essential to electrical machines and is written as

$$e = -k_w N \frac{d}{dt} \int_s B \cdot dS = -k_w N \frac{d\phi}{dt} = -\frac{d\psi}{dt} \quad \dots 1.8$$

Here, we introduce the flux linkage $\psi = k_w N \phi = LI$, one of the core concepts of electrical engineering. It may be noted that the inductance L describes the ability of a coil to produce flux linkage ψ . Later, when calculating the inductance, the effective turns, the permeance Λ or the

reluctance R_m of the magnetic circuit are needed ($L = (k_w N)^2 \Lambda = (k_w N)^2 / R_m$).

❖ **Ampere's law (Equation 1.4)** :- It involves a displacement current that can be given as the time derivative of the electric flux ψ .

Ampere's law

$$\oint_l H \cdot dl = \int_s J \cdot dS + \frac{d}{dt} \int_s D \cdot dS = i(t) + \frac{d\psi_e}{dt} \quad \dots 1.9$$

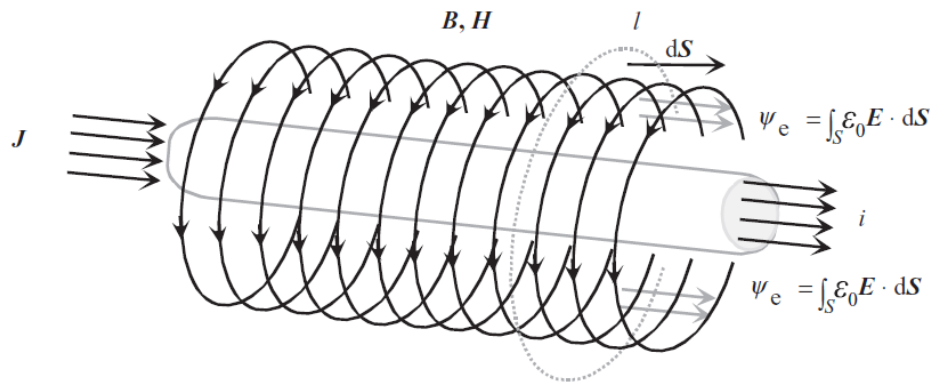


Figure : 1.3

indicates that a current $i(t)$ penetrating a surface S and including the change of electric flux has to be equal to the line integral of the magnetic flux H along the line l around the surface S . Figure 1.3 depicts an application of Ampere's law. The term

$$\frac{d}{dt} \int_s D \cdot dS = \frac{d\psi_e}{dt}$$

in (1.9) is known as Maxwell's displacement current, which ultimately links the electromagnetic phenomena together. The displacement current is Maxwell's historical contribution to the theory of electromagnetism. The invention of displacement current helped him to explain the propagation of electromagnetic waves in a vacuum in the absence of charged particles or currents. Equation (1.9) is quite often presented in its static or quasi-static form, which yields

$$\oint_l H \cdot dl = \int_s J \cdot dS = \sum i(t) = \Theta(t) \quad \dots 1.10$$

The term 'quasi-static' indicates that the frequency f of the phenomenon in question is low enough to neglect Maxwell's

displacement current. The phenomena occurring in electrical machines meet the quasi-static requirement well, since, in practice, considerable displacement currents appear only at radio frequencies or at low frequencies in capacitors that are deliberately produced to take advantage of the displacement currents.

The quasi-static form of Ampere's law is a very important equation in electrical machine design. It is employed in determining the magnetic voltages of an electrical machine and the required current linkage. The instantaneous value of the current sum $\sum i(t)$ in Equation (1.10), that is the instantaneous value of current linkage Θ , can, if desired, be assumed to involve also the apparent current linkage of a permanent magnet $\Theta_{PM} = H'_c h_{PM}$. Thus, the apparent current linkage of a permanent magnet depends on the calculated coercive force H'_c of the material and on the thickness h_{PM} of the magnetic material.

The corresponding differential form of Ampere's law (1.10) in a quasi-static state (dD/dt neglected) is written as

$$\nabla \times H = J \quad \dots 1.11$$

The continuity Equation (1.2) for current density in a quasi-static state is written as

$$\nabla \cdot J = 0 \quad \dots 1.12$$

❖ **Gauss's law for electric fields (Equation 3) :-** In integral form

$$\oint_S D \cdot dS = \int_V \rho_v dV \quad \dots 1.13$$

It indicates that a charge inside a closed surface S that surrounds a volume V creates an electric flux density \mathbf{D} through the surface. Here $\int_V \rho_v dV = q(t)$ is the instantaneous net charge inside the closed surface S . Thus, we can see that in electric fields, there are both sources and drains. When considering the insulation of electrical machines, Equation (1.13) is required. However, in electrical machines, it is not uncommon that charge densities in a medium prove to be zero.

In that case, Gauss's law for electric fields is rewritten as

$$\oint D \cdot dS = 0 \quad \text{or} \quad \nabla \cdot D = 0 \Rightarrow \nabla \cdot E = 0 \quad \dots 1.14$$

In uncharged areas, there are no sources or drains in the electric field either.

❖ **Gauss's law for magnetic fields (Equation 4) :-** In integral form

$$\oint_S B \cdot dS = 0 \quad \dots 1.15$$

states correspondingly that the sum of a magnetic flux penetrating a closed surface S is zero; in other words, the flux entering an object must also leave the object. This is an alternative way of expressing that there is no source for a magnetic flux. In electrical machines, this means for instance that the main flux encircles the magnetic circuit of the machine without a starting or end point. Similarly, all other flux loops in the machine are closed. Figure 1.4 illustrates the surfaces S employed in integral forms of Maxwell's equations, and Figure 1.5, respectively, presents an application of Gauss's law for a closed surface S.

The permittivity, permeability and conductivity ϵ , μ and σ of the medium determine the dependence of the electric and magnetic flux densities and current density on the field strength. In certain cases, ϵ , μ and σ can be treated as simple constants; then the corresponding pair of quantities (D and E, B and H, or J and E) are parallel. Media of this kind are called isotropic, which means that ϵ , μ and σ have the same values in different directions. Otherwise, the media have different values of the quantities ϵ , μ and σ in different directions, and may therefore be treated as tensors; these media are defined as anisotropic. In practice, the permeability in ferromagnetic materials is always a highly nonlinear function of the field strength H : $\mu = f(H)$.

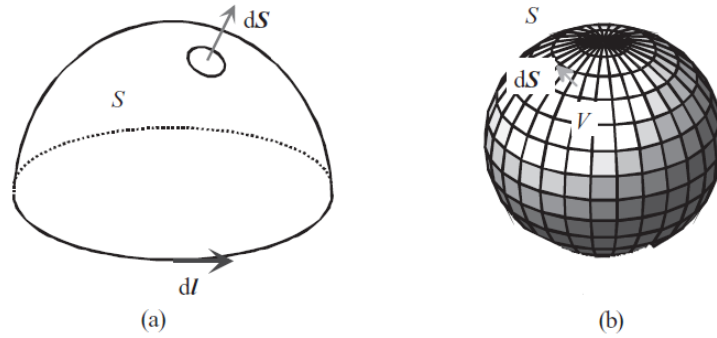


Figure : 1.4

[Surfaces for the integral forms of the equations for electric and magnetic fields.

(a) An open surface S and its contour l ,

(b) a closed surface S , enclosing a volume V . dS is a differential surface vector that is everywhere normal to the surface.]

The general formulations for the equations of a medium can in principle be written as

$$D = f(E) \quad \dots 1.16$$

$$B = f(H) \quad \dots 1.17$$

$$J = f(E) \quad \dots 1.18$$

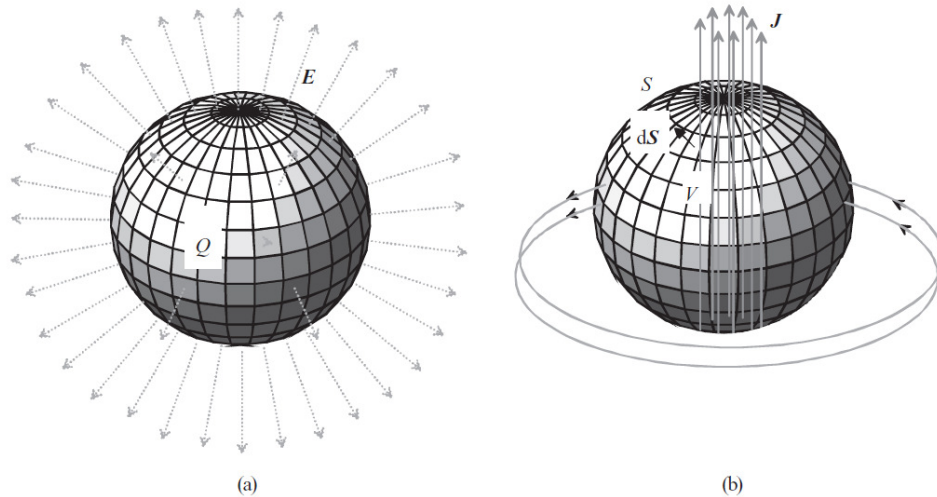


Figure : 1.5

[Illustration of Gauss's law for

(a) an electric field and

(b) a magnetic field. The charge Q inside a closed object acts as a source and creates an electric flux with the field strength \mathbf{E} . Correspondingly, a magnetic flux created by the current density \mathbf{J} outside a closed surface S passes through the closed surface (penetrates into the sphere and then comes out). The magnetic field is thereby source-less ($\text{div}\mathbf{B} = 0$)]

The specific forms for the equations have to be determined empirically for each medium in question. By applying permittivity ϵ [F/m], permeability μ [V s/Am] and conductivity σ [S/m], we can describe materials by the following equations:

$$D = \epsilon E \quad \dots 1.19$$

$$B = \mu H \quad \dots 1.20$$

$$J = \sigma E \quad \dots 1.21$$

Here we see that the displacement current is insignificant from the viewpoint of the machine's basic functionality. However, when a motor is supplied by a frequency converter and the transistors create high frequencies, significant displacement currents may run across the insulation and bearing current problems, for instance, may occur.

1.2 Numerical Solution

The basic design of an electrical machine, that is the dimensioning of the magnetic and electric circuits, is usually carried out by applying analytical equations. However, accurate performance of the machine is usually evaluated using different numerical methods. With these numerical methods, the effect of a single parameter on the dynamical performance of the machine can be effectively studied. Furthermore, some tests, which are not even feasible in laboratory circumstances, can be virtually performed. The most widely used numerical method is the finite element method (FEM), which can be used in the analysis of two- or three-dimensional electromagnetic field problems. The solution can be obtained for static, time-harmonic or transient problems. In the latter two cases, the electric circuit describing the power supply of the machine is coupled with the actual field solution. When applying FEM in the electromagnetic analysis of an electrical machine, special attention has to be paid to the relevance of the electromagnetic material data of the structural parts of the machine as well as to the construction of the finite element mesh.

Because most of the magnetic energy is stored in the air gap of the machine and important torque calculation formulations are related

to the air-gap field solution, the mesh has to be sufficiently dense in this area. The rule of thumb is that the air-gap mesh should be divided into three layers to achieve accurate results. In the transient analysis, that is in time-stepping solutions, the selection of the size of the time step is also important in order to include the effect of high-order time harmonics in the solution. A general method is to divide one time cycle into 400 steps, but the division could be even denser than this, in particular with high-speed machines.

There are five common methods to calculate the torque from the FEM field solution. The solutions are

- (1) the Maxwell stress tensor method,
- (2) Arkkio's method,
- (3) the method of magnetic co-energy differentiation,
- (4) Coulomb's virtual work and
- (5) the magnetizing current method.

The magnetic fields of electrical machines can often be treated as a two-dimensional case, and therefore it is quite simple to employ the magnetic vector potential in the numerical solution of the field. In many cases, however, the fields of the machine are clearly three dimensional, and therefore a two-dimensional solution is always an approximation. In the following, first, the full three-dimensional vector equations are applied.

The magnetic vector potential A is given by

$$B = \nabla \times A \quad \dots 1.22$$

Coulomb's condition, required to define unambiguously the vector potential, is written as

$$\nabla \cdot A = 0 \quad \dots 1.23$$

The substitution of the definition for the magnetic vector potential in the induction law (1.3) yields

$$\nabla \times E = -\nabla \times \frac{\partial}{\partial t} A \quad \dots 1.24$$

Electric field strength can be expressed by the vector potential A and the scalar electric potential ϕ as

$$E = -\frac{\partial A}{\partial t} - \nabla \phi \quad \dots 1.25$$

where ϕ is the reduced electric scalar potential. Because $\nabla \times \nabla \phi \equiv 0$, adding a scalar potential causes no problems with the induction law. The equation shows that the electric field strength vector consists of two parts, namely a rotational part induced by the time dependence of the magnetic field, and a non-rotational part created by electric charges and the polarization of dielectric materials.

Current density depends on the electric field strength

$$J = \sigma E = -\sigma \frac{\partial A}{\partial t} - \sigma \nabla \phi \quad \dots 1.26$$

Ampere's law and the definition for vector potential yield

$$\nabla \times \left(\frac{1}{\mu} \nabla \times A \right) = J \quad \dots 1.27$$

Substituting (1.26) into (1.27) gives

$$\nabla \times \left(\frac{1}{\mu} \nabla \times A \right) + \sigma \frac{\partial A}{\partial t} + \sigma \nabla \phi = 0 \quad \dots 1.28$$

The latter is valid in areas where eddy currents may be induced, whereas the former is valid in areas with source currents $J = J_s$, such as winding currents, and areas without any current densities $J = 0$.

In electrical machines, a two-dimensional solution is often the obvious one; in these cases, the numerical solution can be based on a single component of the vector potential A . The field solution (B , H) is found in an x - y plane, whereas J , A and E involve only the z -component. The gradient $\nabla \phi$ only has a z -component, since J and A are parallel to z , and (1.26) is valid. The reduced scalar potential is thus independent of x - and y -components. ϕ could be a linear function of the z -coordinate, since a two-dimensional field solution is independent of z . The assumption of two-dimensionality is not valid if there are potential differences caused by electric charges or by the polarization of

insulators. For two-dimensional cases with eddy currents, the reduced scalar potential has to be set as $\varphi = 0$.

In a two-dimensional case, the previous equation is rewritten as

$$-\nabla \cdot \left(\frac{1}{\mu} \nabla A_z \right) + \sigma \frac{\partial A_z}{\partial t} = 0 \quad \dots 1.29$$

Outside eddy current areas, the following is valid:

$$-\nabla \cdot \left(\frac{1}{\mu} \nabla A_z \right) = J_z \quad \dots 1.30$$

The definition of vector potential yields the following components for flux density:

$$B_x = \frac{\partial A_z}{\partial y}, B_y = -\frac{\partial A_z}{\partial x} \quad \dots 1.31$$

Hence, the vector potential remains constant in the direction of the flux density vector. Consequently, the iso-potential curves of the vector potential are flux lines. In the two-dimensional case, the following formulation can be obtained from the partial differential equation of the vector potential:

$$-k \left[\frac{\partial}{\partial x} \left(\nu \frac{\partial A_z}{\partial x} \right) + \frac{\partial}{\partial y} \left(\nu \frac{\partial A_z}{\partial y} \right) \right] = kJ \quad \dots 1.32$$

Here ν is the reluctivity of the material. This again is similar to the equation for a static electric field

$$\nabla \cdot (\nu \nabla A) = -J \quad \dots 1.33$$

Further, there are two types of boundary conditions. Dirichlet's boundary condition indicates that a known potential, here the known vector potential

$$A = \text{constant} \quad \dots 1.34$$

can be achieved for a vector potential for instance on the outer surface of an electrical machine. The field is parallel to the contour of the surface. Similar to the outer surface of an electrical machine, also the centre line of the machine's pole can form a symmetry plane. Neumann's homogeneous boundary condition determined with the vector potential

$$v \frac{\partial A}{\partial n} = 0 \quad \dots 1.35$$

can be achieved when the field meets a contour perpendicularly. Here n is the normal unit vector of a plane. A contour of this kind is for instance part of a field confined to infinite permeability iron or the centre line of the pole clearance.

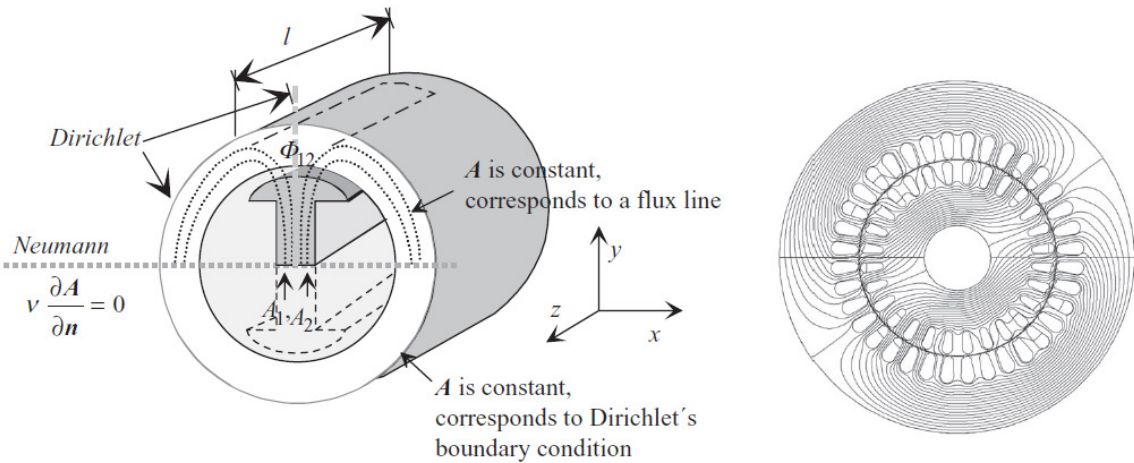


Figure : 1.6

[Left, a two-dimensional field and its boundary conditions for a salient-pole synchronous machine are illustrated. Here, the constant value of the vector potential A (e.g. the machine's outer contour) is taken as Dirichlet's boundary condition, and the zero value of the derivative of the vector potential with respect to normal is taken as Neumann's boundary condition. In the case of magnetic scalar potential, the boundary conditions with respect to potential would take opposite positions. Because of symmetry, the zero value of the normal derivative of the vector potential corresponds to the constant magnetic potential V_m , which in this case would be a known potential and thus Dirichlet's boundary condition.

Right, a vector-potential-based field solution of a two-pole asynchronous machine assuming a two-dimensional field is presented]

The magnetic flux penetrating a surface is easy to calculate with the vector potential. Stoke's theorem yields for the flux

$$\phi = \int_s B \cdot dS = \int_s (\nabla \times A) \cdot dS = \oint_l A \cdot dl \quad \dots 1.36$$

This is an integral around the contour l of the surface S . These phenomena are illustrated with Figure 1.6. In the two-dimensional case of the illustration, the end faces' share of the integral is zero, and the vector potential along the axis is constant. Consequently, for a machine of length l we obtain a flux

$$\phi_{12} = l(A_1 - A_2) \quad \dots 1.37$$

This means that the flux ϕ_{12} is the flux between vector equipotential lines A_1 and A_2 .

2.

The Finite Element Method :-

The finite element method (FEM) has its origin in the field of structural analysis. The method was not applied to EM problems until 1968. Like the finite difference method, the finite element method is useful in solving differential equations. The finite difference method represents the solution region by an array of grid points; its application becomes difficult with problems having irregularly shaped boundaries. Such problems can be handled more easily using the finite element method.

The finite element analysis of any problem involves basically four steps:

- (a) discretizing the solution region into a finite number of sub-regions or *elements*,
- (b) deriving governing equations for a typical element,
- (c) assembling of all elements in the solution region, and
- (d) solving the system of equations obtained.

2.1 Finite Element Discretization

We divide the solution region into a number of *finite elements* as illustrated in Figure 2.1 where the region is subdivided into four non-overlapping elements (two triangular and two quadrilateral) and seven nodes. We seek an approximation for the potential V_e within an

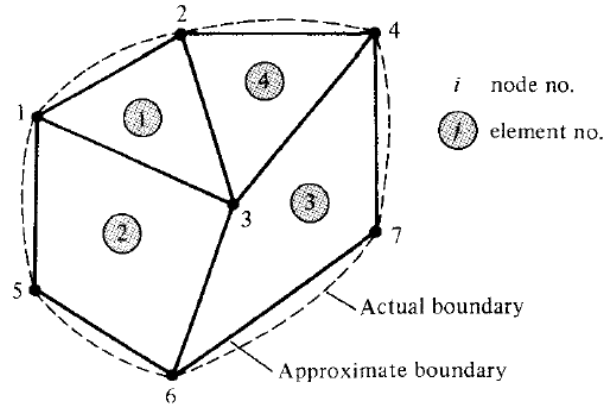


Figure 2.1

A typical finite element sub-division of an irregular domain

element e and then interrelate the potential distributions in various elements such that the potential is continuous across inter-element boundaries. The approximate solution for the whole region is

$$V(x, y) \approx \sum_{e=1}^N V_e(x, y) \quad \dots 2.1$$

where N is the number of triangular elements into which the solution region is divided.

The most common form of approximation for V_e within an element is polynomial approximation, namely

$$V_e(x, y) = a + bx + cy \quad \dots 2.2$$

for a triangular element and

$$V_e(x, y) = a + bx + cy + dxy \quad \dots 2.3$$

for a quadrilateral element. The potential V_e in general is nonzero within element e but zero outside e . It is difficult to approximate the boundary of the solution region with quadrilateral elements; such elements are useful for problems whose boundaries are sufficiently regular. In view of this, we prefer to use triangular elements throughout our analysis in

this section. Notice that our assumption of linear variation of potential within the triangular element as in eq. (2.2) is the same as assuming that the electric field is uniform within the element; that is,

$$E_e = -\nabla V_e = -(ba_x + ca_y) \quad \dots 2.4$$

2.2 Element Governing Equations

Consider a typical triangular element shown in Figure 2.2. The potential V_{e1} , V_{e2} and V_{e3} at nodes 1, 2, and 3, respectively, are obtained using eq. (2.2); that is,

$$\begin{bmatrix} V_{e1} \\ V_{e2} \\ V_{e3} \end{bmatrix} = \begin{bmatrix} 1 & x_1 & y_1 \\ 1 & x_2 & y_2 \\ 1 & x_3 & y_3 \end{bmatrix} \begin{bmatrix} a \\ b \\ c \end{bmatrix} \quad \dots 2.5$$

The coefficients a , b , and c are determined from eq. (2.5) as

$$\begin{bmatrix} a \\ b \\ c \end{bmatrix} = \begin{bmatrix} 1 & x_1 & y_1 \\ 1 & x_2 & y_2 \\ 1 & x_3 & y_3 \end{bmatrix}^{-1} \begin{bmatrix} V_{e1} \\ V_{e2} \\ V_{e3} \end{bmatrix} \quad \dots 2.6$$

Substituting this into eq. (2.2) gives

$$V_e = [1 \quad x \quad y] \frac{1}{2A} \begin{bmatrix} (x_2 y_3 - x_3 y_2) & (x_3 y_1 - x_1 y_3) & (x_1 y_2 - x_2 y_1) \\ (y_2 - y_3) & (y_3 - y_1) & (y_1 - y_2) \\ (x_3 - x_2) & (x_1 - x_3) & (x_2 - x_1) \end{bmatrix} \begin{bmatrix} V_{e1} \\ V_{e2} \\ V_{e3} \end{bmatrix}$$

or

$$V_e = \sum_{i=1}^3 \alpha_i(x, y) V_{ei} \quad \dots 2.7$$

A is the area of the element e ; that is

$$2A = \begin{vmatrix} 1 & x_1 & y_1 \\ 1 & x_2 & y_2 \\ 1 & x_3 & y_3 \end{vmatrix}$$

$$= (x_1y_2 - x_2y_1) + (x_3y_1 - x_1y_3) + (x_2y_3 - x_3y_2)$$

or

$$A = 1/2 [(x_2 - x_1)(y_3 - y_1) - (x_3 - x_1)(y_2 - y_1)] \quad \dots 2.8$$

The value of A is positive if the nodes are numbered counterclockwise (starting from any node) as shown by the arrow in Figure 2.2. Note that eq. (2.7) gives the potential at any point (x, y) within the element provided that the potentials at the vertices are known. This is unlike the situation in finite difference analysis where the potential is known at the grid points only. Also note that α_i are linear interpolation functions. They are called the element shape functions and they have the following properties:

$$\alpha_i(x_j, y_j) = \begin{cases} 1, & i = j \\ 0, & i \neq j \end{cases} \quad \dots 2.9a$$

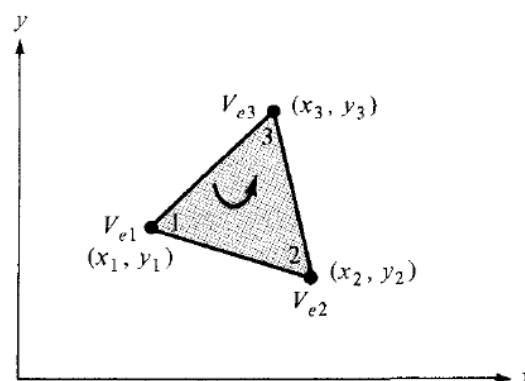


Figure 2.2

Typical triangular element; the local node numbering 1-2-3 must be counterclockwise as indicated by the arrow.

$$\sum_{i=1}^3 \alpha_i(x, y) = 1 \quad \dots 2.9b$$

The shape functions α_1 and α_2 , for example, are illustrated in Figure 2.3. The energy per unit length associated with the element e is given by

$$W_e = \frac{1}{2} \int \epsilon |E|^2 dS = \frac{1}{2} \int \epsilon |\nabla V_e|^2 dS \quad \dots 2.10$$

where a two-dimensional solution region free of charge ($\rho_s = 0$) is assumed. But from eq. (2.7),

$$\nabla V_e = \sum_{i=1}^3 V_{ei} \nabla \alpha_i \quad \dots 2.11$$

Substituting eq. (2.11) into eq. (2.10) gives

$$W_e = \frac{1}{2} \sum_{i=1}^3 \sum_{j=1}^3 \epsilon V_{ei} \left[\int \nabla \alpha_i \cdot \nabla \alpha_j dS \right] V_{ej} \quad \dots 2.12$$

If we define the term in brackets as

$$C_{ij}^{(e)} = \int \nabla \alpha_i \cdot \nabla \alpha_j dS \quad \dots 2.13$$

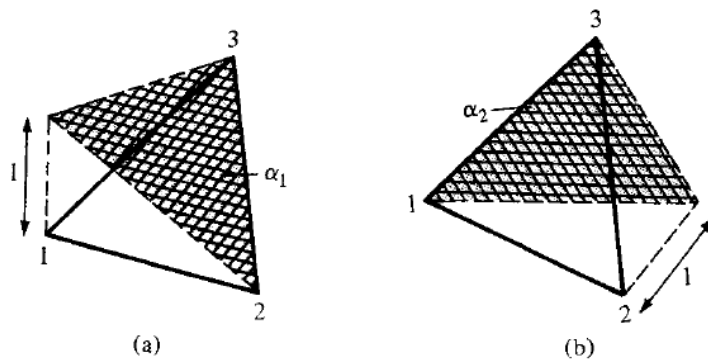


Figure 2.3

Shape functions a_1 , and a_2 for a triangular element.

we may write eq. (2.12) in matrix form as

$$W_e = \frac{1}{2} \boldsymbol{\varepsilon} [V_e]^T [C^{(e)}] [V_e] \quad \dots 2.14$$

where the superscript T denotes the transpose of the matrix,

$$[V_e] = \begin{bmatrix} V_{e1} \\ V_{e2} \\ V_{e3} \end{bmatrix} \quad \dots 2.15a$$

and

$$[C^{(e)}] = \begin{bmatrix} C_{11}^{(e)} & C_{12}^{(e)} & C_{13}^{(e)} \\ C_{21}^{(e)} & C_{22}^{(e)} & C_{23}^{(e)} \\ C_{31}^{(e)} & C_{32}^{(e)} & C_{33}^{(e)} \end{bmatrix} \quad \dots 2.15b$$

The matrix $C^{(e)}$ is usually called the *element coefficient matrix*. The matrix element $C_{ij}^{(e)}$ of the coefficient matrix may be regarded as the coupling between nodes i and j ; its value is obtained from eqs. (2.8) and (2.13). For example,

$$\begin{aligned} C_{12}^{(e)} &= \int \nabla \alpha_1 \cdot \nabla \alpha_2 dS \\ &= \frac{1}{4A^2} [(y_2 - y_3)(y_3 - y_1) + (x_3 - x_2)(x_1 - x_3)] \int dS \\ &= \frac{1}{4A} [(y_2 - y_3)(y_3 - y_1) + (x_3 - x_2)(x_1 - x_3)] \quad \dots 2.16a \end{aligned}$$

Similarly :

$$C_{11}^{(e)} = \frac{1}{4A} \left[(y_2 - y_3)^2 + (x_3 - x_2)^2 \right] \quad \dots 2.16b$$

$$C_{13}^{(e)} = \frac{1}{4A} \left[(y_2 - y_3)(y_1 - y_2) + (x_3 - x_2)(x_2 - x_1) \right] \quad \dots 2.16c$$

$$C_{22}^{(e)} = \frac{1}{4A} \left[(y_2 - y_3)^2 + (x_1 - x_3)^2 \right] \quad \dots 2.16d$$

$$C_{23}^{(e)} = \frac{1}{4A} \left[(y_3 - y_1)(y_1 - y_2) + (x_1 - x_3)(x_2 - x_1) \right] \quad \dots 2.16e$$

$$C_{33}^{(e)} = \frac{1}{4A} \left[(y_1 - y_2)^2 + (x_2 - x_1)^2 \right] \quad \dots 2.16f$$

Also

$$C_{21}^{(e)} = C_{12}^{(e)} \quad , \quad C_{31}^{(e)} = C_{13}^{(e)} \quad , \quad C_{32}^{(e)} = C_{23}^{(e)} \quad \dots 2.16g$$

However, our calculations will be easier if we define

$$P_1 = (y_2 - y_3) \quad , \quad P_2 = (y_3 - y_1) \quad , \quad P_3 = (y_1 - y_2)$$

$$Q_1 = (x_3 - x_2) \quad , \quad Q_2 = (x_1 - x_3) \quad , \quad Q_3 = (x_2 - x_1) \quad \dots 2.17a$$

With P_i and Q_i ($i = 1, 2, 3$ are the local node numbers), each term in the element coefficient matrix is found as

$$C_{ij}^{(e)} = \frac{1}{4A} \left[P_i P_j + Q_i Q_j \right] \quad \dots 2.17b$$

where

$$A = \frac{1}{2} (P_2 Q_3 - P_3 Q_2) \quad \dots 2.17c$$

Note that $P_1 + P_2 + P_3 = 0 = Q_1 + Q_2 + Q_3$ and hence $\sum_{i=1}^3 C_{ij}^{(e)} = 0 = \sum_{j=1}^3 C_{ij}^{(e)}$.

This may be used in checking our calculations.

2.3 Assembling of All Elements

Having considered a typical element, the next step is to assemble all such elements in the solution region. The energy associated with the assemblage of all elements in the mesh is

$$W = \sum_{e=1}^N W_e = \frac{1}{2} \boldsymbol{\varepsilon} [V]^T [C][V] \quad \dots 2.18$$

where

$$[V] = \begin{bmatrix} V_1 \\ V_2 \\ \cdot \\ \cdot \\ V_n \end{bmatrix} \quad \dots 2.19$$

n is the number of nodes, N is the number of elements, and $[C]$ is called the overall or global coefficient matrix, which is the assemblage of individual element coefficient matrices. The major problem now is obtaining $[C]$ from $[C^{(e)}]$.

The process by which individual element coefficient matrices are assembled to obtain the global coefficient matrix is best illustrated with an example. Consider the finite element mesh consisting of three finite elements as shown in Figure 2.4. Observe the numberings of the nodes. The numbering of nodes as 1, 2, 3, 4, and 5 is called global numbering. The numbering i - j - k is called local numbering and it corresponds with 1-2-3 of the element in

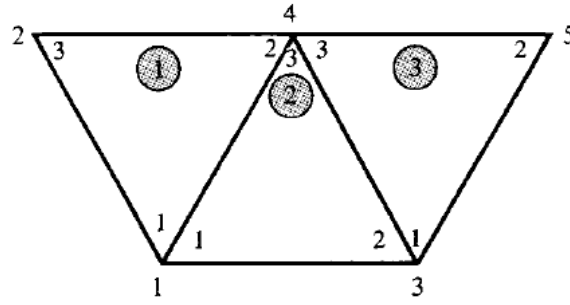


Figure 2.4

Assembly of three elements: $i-j-k$ corresponds to local numbering 1 -2-3 of the element in Figure 2.2.

Figure 2.2. For example, for element 3 in Figure 2.4, the global numbering 3-5-4 corresponds with local numbering 1-2-3 of the element in Figure 2.2. Note that the local numbering must be in counterclockwise sequence starting from any node of the element. For element 3, for example, we could choose 4-3-5 or 5-4-3 instead of 3-5-4 to correspond with 1-2-3 of the element in Figure 2.2. Thus the numbering in Figure 2.4 is not unique. However, we obtain the same $[C]$ whichever numbering is used. Assuming the particular numbering in Figure 2.4, the global coefficient matrix is expected to have the form

$$[C] = \begin{bmatrix} C_{11} & C_{12} & C_{13} & C_{14} & C_{15} \\ C_{21} & C_{22} & C_{23} & C_{24} & C_{25} \\ C_{31} & C_{32} & C_{33} & C_{34} & C_{35} \\ C_{41} & C_{42} & C_{43} & C_{44} & C_{45} \\ C_{51} & C_{52} & C_{53} & C_{54} & C_{55} \end{bmatrix} \quad \dots \text{ 2.20}$$

which is a 5 X 5 matrix since five nodes ($n = 5$) are involved. Again, C_{ij} is the coupling between nodes i and j . We obtain C_y by utilizing the fact that the potential distribution must be continuous across inter-element boundaries. The contribution to the i, j position in $[C]$ comes from all elements containing nodes i and j . To find C_u , for example, we observe from Figure 2.4 that global node 1 belongs to elements 1 and 2 and it is local node 1 in both; hence,

$$C_{11} = C_{11}^{(1)} + C_{11}^{(2)} \quad \dots 2.21a$$

For C_{22} , global node 2 belongs to element 1 only and is the same as local node 3; hence,

$$C_{22} = C_{33}^{(1)} \quad \dots 2.21b$$

For C_{44} , global node 4 is the same as local nodes 2, 3, and 3 in elements 1, 2, and 3, respectively; hence,

$$C_{44} = C_{22}^{(1)} + C_{11}^{(2)} + C_{33}^{(3)} \quad \dots 2.21c$$

For C_{14} , global link 14 is the same as the local links 12 and 13 in elements 1 and 2, respectively; hence,

$$C_{14} = C_{12}^{(1)} + C_{13}^{(2)} \quad \dots 2.21d$$

Since there is no coupling (or direct link) between nodes 2 and 3,

$$C_{23} = C_{32} = 0 \quad \dots 2.21e$$

Continuing in this manner, we obtain all the terms in the global coefficient matrix by inspection of Figure 2.4 as

$$[C] = \begin{bmatrix} C_{11}^{(1)} + C_{11}^{(2)} & C_{13}^{(1)} & C_{12}^{(2)} & C_{12}^{(1)} + C_{13}^{(2)} & 0 \\ C_{31}^{(1)} & C_{33}^{(1)} & 0 & C_{32}^{(1)} & 0 \\ C_{21}^{(2)} & 0 & C_{22}^{(2)} + C_{11}^{(3)} & C_{23}^{(2)} + C_{13}^{(3)} & C_{12}^{(3)} \\ C_{21}^{(1)} + C_{31}^{(2)} & C_{23}^{(1)} & C_{32}^{(2)} + C_{31}^{(3)} & C_{22}^{(1)} + C_{33}^{(2)} + C_{33}^{(3)} & C_{32}^{(3)} \\ 0 & 0 & C_{21}^{(3)} & C_{23}^{(3)} & C_{22}^{(3)} \end{bmatrix} \quad \dots 2.22$$

The element coefficient matrices overlap at nodes shared by elements and that there are 27 terms (nine for each of the three elements) in the global coefficient matrix $[C]$. Also note the following properties of the matrix $[C]$:

1. It is symmetric ($C_{ij} = C_{ji}$) just as the element coefficient matrix.

2. Since $C_{ij} = 0$ if no coupling exists between nodes i and j , it is evident that for a large number of elements $[C]$ becomes sparse and banded.
3. It is singular. Although this is not so obvious, it can be shown using the element coefficient matrix of eq. (2.15b).

2.4 Solving the Resulting Equations :-

From variational calculus, it is known that Laplace's (or Poisson's) equation is satisfied when the total energy in the solution region is minimum. Thus we require that the partial derivatives of W with respect to each nodal value of the potential be zero; that is,

$$\frac{\partial W}{\partial V_1} = \frac{\partial W}{\partial V_2} = \dots = \frac{\partial W}{\partial V_n} = 0$$

or

$$\frac{\partial W}{\partial V_k} = 0, k = 1, 2, \dots, n \quad \dots 2.23$$

For example, to get $\frac{\partial W}{\partial V_1} = 0$ for the finite element mesh of Figure 15.29,

we substitute eq. (15.65) into eq. (15.63) and take the partial derivative of W with respect to V_1 . We obtain

$$0 = \frac{\partial W}{\partial V_1} = 2V_1C_{11} + V_2C_{12} + V_3C_{13} + V_4C_{14} + V_5C_{15} + V_2C_{21} + V_3C_{31} + V_4C_{41} + V_5C_{51}$$

or

$$0 = V_1C_{11} + V_2C_{12} + V_3C_{13} + V_4C_{14} + V_5C_{15} \quad \dots 2.24$$

In general, $\frac{\partial W}{\partial V_k} = 0$ leads to

$$0 = \sum_{i=1}^n V_i C_{ki} \quad \dots 2.25$$

where n is the number of nodes in the mesh. By writing eq. (2.25) for all nodes $k = 1, 2, \dots, n$, we obtain a set of simultaneous equations from which the solution of $[V]^T = [V_1, V_2, \dots, V_n]$ can be found. This can be done in two ways similar to those used in solving finite difference equations obtained from Laplace's (or Poisson's) equation.

Iteration Method :

This approach is similar to that used in finite difference method. Let us assume that node 1 in Figure 2.4, for example, is a free node. The potential at node 1 can be obtained from eq. (2.24) as

$$V_1 = -\frac{1}{C_{11}} \sum_{i=2}^5 V_i C_{1i} \quad \dots 2.26$$

In general, the potential at a free node k is obtained from eq. (2.25) as

$$V_k = -\frac{1}{C_{kk}} \sum_{i=1, i \neq k}^n V_i C_{ik} \quad \dots 2.27$$

This is applied iteratively to all the free nodes in the mesh with n nodes. Since $C_{ki} = 0$ if node k is not directly connected to node i , only nodes that are directly linked to node k contribute to V_k in eq. (2.27).

Thus if the potentials at nodes connected to node k are known, we can determine V_k using eq. (2.27). The iteration process begins by setting the potentials at the free nodes equal to zero or to the average potential.

$$V_{avg} = \frac{1}{2} (V_{min} + V_{max}) \quad \dots 2.28$$

where V_{min} and V_{max} are the minimum and maximum values of the prescribed potentials at the fixed nodes. With those initial values, the potentials at the free nodes are calculated using eq. (2.27). At the end of the first iteration, when the new values have been calculated for all the free nodes, the values become the old values for the second iteration.

The procedure is repeated until the change between subsequent iterations becomes negligible.

Band Matrix Method :

If all free nodes are numbered first and the fixed nodes last, eq. (2.18) can be written such that

$$W = \frac{1}{2} \varepsilon \begin{bmatrix} V_f & V_p \end{bmatrix} \begin{bmatrix} C_{ff} & C_{fp} \\ C_{pf} & C_{pp} \end{bmatrix} \begin{bmatrix} V_f \\ V_p \end{bmatrix} \quad \dots 2.29$$

where subscripts f and p , respectively, refer to nodes with free and fixed (or prescribed) potentials. Since V_p is constant (it consists of known, fixed values), we only differentiate with respect to V_f so that applying eq. (2.23) to eq. (2.29) yields

$$C_{ff} V_p + C_{fp} V_p = 0$$

or

$$\begin{bmatrix} C_{ff} \end{bmatrix} \begin{bmatrix} V_f \end{bmatrix} = - \begin{bmatrix} C_{fp} \end{bmatrix} \begin{bmatrix} V_p \end{bmatrix} \quad \dots 2.30$$

This equation can be written as

$$[A][V] = [B] \quad \dots 2.31a$$

or

$$[V] = [A]^{-1} [B] \quad \dots 2.31b$$

where $[V] = [V_f]$, $[A] = [C_{ff}]$, and $[B] = -[C_{fp}][V_p]$. Since $[A]$ is, in general, non-singular, the potential at the free nodes can be found using eq. (2.30). We can solve for $[V]$ in eq. (2.31a) using Gaussian elimination technique. We can also solve for $[V]$ in eq. (2.31b) using matrix inversion if the size of the matrix to be inverted is not large.

Notice that as from eq. (2.10) onward, our solution has been restricted to a two-dimensional problem involving Laplace's equation, $\nabla^2 V = 0$. The basic concepts developed in this section can be extended to finite element analysis of problems involving Poisson's equation $\left(\nabla^2 V = -\frac{\rho_v}{\epsilon}, \nabla^2 A = -\mu J \right)$ or wave equation $(\nabla^2 \phi - \gamma^2 \phi = 0)$. A major problem associated with finite element analysis is the relatively large amount of computer memory required in storing the matrix elements and the associated computational time. However, several algorithms have been developed to alleviate the problem to some degree.

The finite element method (FEM) has a number of advantages over the finite difference method (FDM) and the method of moments (MOM). First, the FEM can easily handle complex solution region. Second, the generality of FEM makes it possible to construct a general-purpose program for solving a wide range of problems. A single program can be used to solve different problems (described by the same partial differential equations) with different solution regions and different boundary conditions; only the input data to the problem need be changed. However, FEM has its own drawbacks. It is harder to understand and program than FDM and MOM. It also requires preparing input data, a process that could be tedious.

3.

Permanent Magnet Materials

3.1 Demagnetization curve and magnetic parameters

A *permanent magnet* (PM) can produce magnetic field in an air gap with no excitation winding and no dissipation of electric power. External energy is involved only in changing the energy of magnetic field, not in maintaining it. As any other ferromagnetic material, a PM can be described by its B-H hysteresis loop. PMs are also called *hard magnetic materials*, meaning ferromagnetic materials with a wide hysteresis loop.

The basis for the evaluation of a PM is the portion of its hysteresis loop located in the upper left-hand quadrant, called the *demagnetization curve* (Fig. 3.1). If a reverse magnetic field intensity is applied to a previously magnetized, say, toroidal specimen, the magnetic flux density drops down to the magnitude determined by the point *K*. When the reversal magnetic flux density is removed, the flux density returns to the point *L* according to a minor hysteresis loop. Thus, the application of a reverse field has reduced the *remanence*, or *remanent magnetism*. Reapplying a magnetic field intensity will again reduce the flux density, completing the minor hysteresis loop by returning the core to approximately the same value of flux density at the point *K* as before. The minor hysteresis loop may usually be replaced with little error by a straight line called the *recoil line*. This line has a slope called the *recoil permeability* μ_{rec} .

As long as the negative value of applied magnetic field intensity does not exceed the maximum value corresponding to the point *K*, the PM may be regarded as being reasonably permanent.

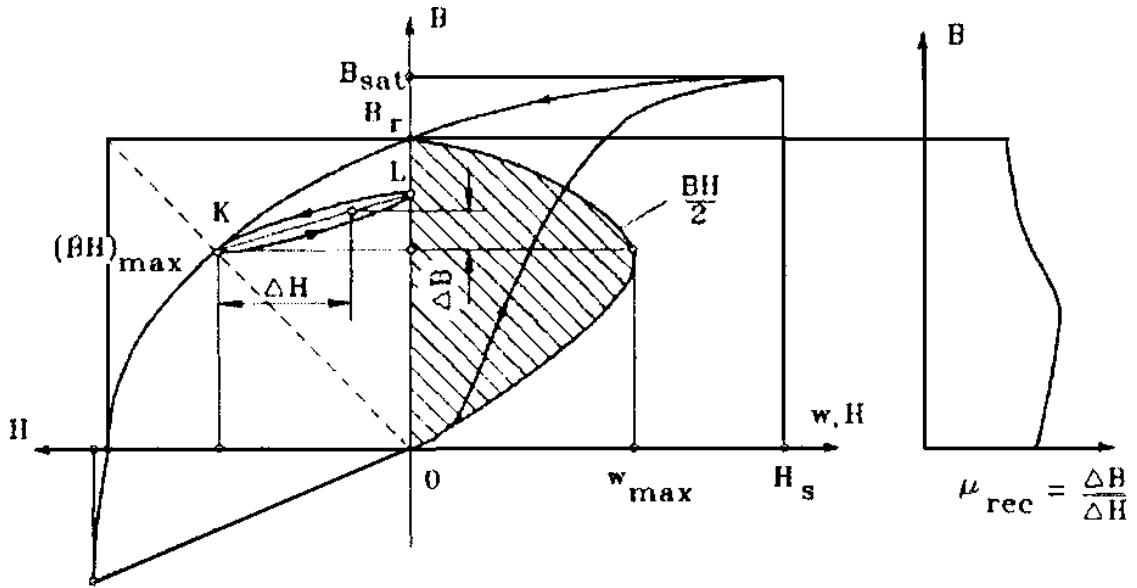


Figure : 3.1

[Demagnetization curve, recoil loop, energy of a PM, and recoil magnetic permeability.]

If, however, a greater negative field intensity H is applied, the magnetic flux density will be reduced to a value lower than that at point K . On the removal of H , a new and lower recoil line will be established.

The general relationship between the magnetic flux density B , intrinsic magnetization B_i due to the presence of the ferromagnetic material, and magnetic field intensity H may be expressed as

$$B = \mu_0 H + B_i = \mu_0 (H + M) = \mu_0 (1 + X) H = \mu_0 \mu_r H \quad \dots 3.1$$

in which $\vec{B}, \vec{H}, \vec{B}_i$ and $\vec{M} = \frac{\vec{B}_i}{\mu_0}$ are parallel or anti-parallel vectors, so that

eqn (3.1) can be written in a scalar form. The magnetic permeability of free space $\mu_0 = 0.4\pi \times 10^{-6}$ H/m. The relative magnetic permeability of ferromagnetic materials $\mu_r = 1 + x \gg 1$. The magnetization vector \vec{M} is proportional to the magnetic susceptibility x of the material. The flux density $\mu_0 H$ would be present within, say, a toroid if the ferromagnetic

core was not in place. The flux density B_i is the contribution of the ferromagnetic core.

PMs are characterized by the parameters listed below.

Saturation magnetic flux density B_{sat} and corresponding saturation magnetic field intensity H_{sat} . At this point the alignment of all the *magnetic moments of domains* is in the direction of the external applied magnetic field.

Remanent magnetic flux density B_r , or **remanence**, is the magnetic flux density corresponding to zero magnetic field intensity. High remanence means the magnet can support higher magnetic flux density in the air gap of the magnetic circuit.

Coercive field strength H_c , or **coercivity**, is the value of demagnetizing field intensity necessary to bring the magnetic flux density to zero in a material previously magnetized (in a symmetrically cyclically magnetized condition). High coercivity means that a thinner magnet can be used to withstand the demagnetization field.

Intrinsic demagnetization curve is the portion of the $B_i = f(H)$ hysteresis loop located in the upper left-hand quadrant, where $B_i = B - \mu_0 H$ is according to eqn (3.1). For $H = 0$ the intrinsic magnetic flux density $B_i = B_r$.

Intrinsic coercivity, H_c' is the magnetic field strength required to bring to zero the intrinsic magnetic flux density B_i of a magnetic material described by the $B_i = f(H)$ curve. For PM materials, $H_c' > H_c$.

Recoil magnetic permeability μ_{rec} is the ratio of the magnetic flux density to magnetic field intensity at any point on the demagnetization curve, i.e.,

$$\mu_{rec} = \mu_0 \mu_{rrec} = \frac{\Delta B}{\Delta H} \quad \dots 3.2$$

where the *relative recoil permeability* $\mu_{rrec} = 1 \dots 3.5$.

Maximum magnetic energy per unit produced by a PM in the external space is equal to the maximum magnetic energy density per volume, i.e.

$$w_{max} = \frac{(BH)_{max}}{2} \text{ J/m}^3 \quad \dots 3.3$$

where the product $(BH)_{max}$ corresponds to the maximum energy density point on the demagnetization curve with coordinates B_{max} and H_{max} .

Form factor of the demagnetization curve characterizes the concave shape of the demagnetization curve, i.e.,

$$\gamma = \frac{(BH)_{max}}{B_r H_c} = \frac{B_{max} H_{max}}{B_r H_c} \quad \dots 3.4$$

For a square demagnetization curve $\gamma=1$ and for a straight line (rare-earth PM) $\gamma=0.25$.

3.2 Early history of permanent magnets :-

A hard magnetic material called *loadstone* was mentioned by Greek philosopher Thales of Miletus as early as ca. 600 B.C. This was a natural magnetic mineral, a form of magnetite Fe_3O_4 . Loadstone was given the name *magnes* because it was found in Magnesia, a district in Thessaly.

The first artificial magnets were iron needles magnetized by touching the loadstone. Man's first practical use of magnetism may have been the compass. Around 1200 A.D. there are references in a French poem written by Guyot de Provins to a touched needle of iron supported by a floating straw. Other references suggest that good magnet steel was available from China in about 500 A.D.

The earliest systematic reporting of magnets was a classical paper by W. Gilbert in 1600. Gilbert described how to arm loadstones with soft iron pole tips to increase attractive force on contact and how to magnetize pieces of iron or steel. The next great advance in magnetism came with the invention of the electromagnet by J. Henry and W. Sturgeon in 1825.

By 1867, German handbooks recorded that ferromagnetic alloys could be made from non-ferromagnetic materials and non-ferromagnetic alloys of ferromagnetic materials, mainly iron. For example in 1901, *Heusler alloys*, which had outstanding properties compared to previous magnets, were reported. The composition of a typical *Heusler* alloy was 10 to 30% manganese and 15 to 19% aluminum, the balance being copper.

In 1917 *cobalt steel alloys* and in 1931 *Alnico* (Al, Ni, Co, Fe) were discovered in Japan. In 1938, also in Japan, Kato and Takei developed magnets made of *powdered oxides*. This development was the forerunner of the modern *ferrite*.

3.3 Properties of permanent magnets :-

There are three classes of PMs currently used for electric motors:

- Alnicos (Al, Ni, Co, Fe);
- Ceramics (ferrites), e.g., barium ferrite $\text{BaO} \cdot 6\text{Fe}_2\text{O}_3$ and strontium ferrite $\text{SrO} \cdot 6\text{Fe}_2\text{O}_3$;
- Rare-earth materials, i.e., samarium-cobalt SmCo and neodymium-iron-boron NdFeB.

Demagnetization curves of the above PM materials are given in Fig. 3.2. Demagnetization curves are sensitive to the temperature. Both B_r and H_c decrease as the magnet temperature increases, i.e.,

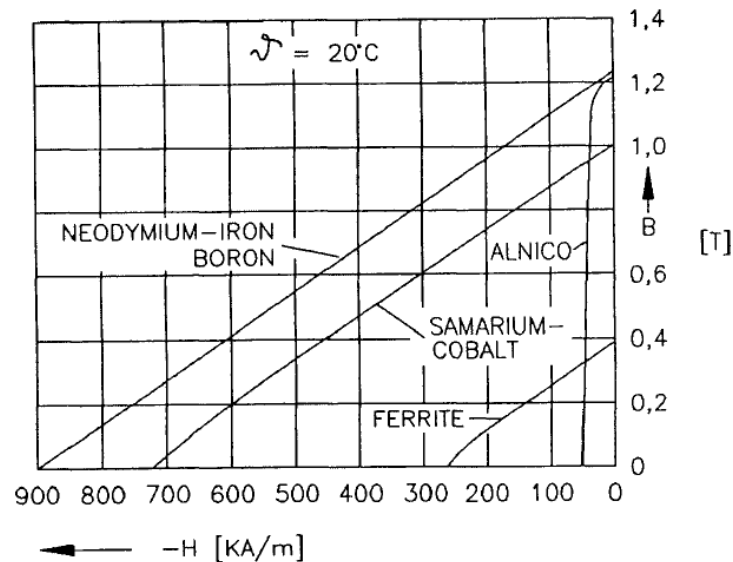


Figure : 3.2

[Demagnetization curves for different permanent magnet materials.]

❖ **Alnico**

The main advantages of *Alnico* are its high magnetic remanent flux density and low temperature coefficients. The temperature coefficient of B_r is $-0.02\%/^\circ\text{C}$ and maximum service temperature is 520°C . These advantages allow a high air gap magnetic flux density at high magnet temperature. Unfortunately, coercive force is very low and the demagnetization curve is extremely non-linear. Therefore, it is very easy not only to magnetize but also to demagnetize Alnico.

Alnico has been used in PM d.c. commutator motors of disk type with relatively large air gaps. This results in a negligible armature reaction magnetic flux acting on the PMs. Sometimes, Alnico PMs are protected from the armature flux, and consequently from demagnetization, using additional mild steel pole shoes. Alnicos dominated the PM motors market in the range from a few watts to 150 kW between the mid 1940s and the late 1960s when ferrites became the most widely used materials .

❖ **Ferrites**

Barium and strontium *ferrites* were invented in the 1950s. A ferrite has a higher coercive force than Alnico, but at the same time has a lower remanent magnetic flux density. Temperature coefficients are relatively high, i.e. the coefficient of B_r is $-0.20\%/^{\circ}\text{C}$ and the coefficient of H_c is $-0.27\%/^{\circ}\text{C}$. The maximum service temperature is 400°C . The main advantages of ferrites are their low cost and very high electric resistance, which means no eddy-current losses in the PM volume.

Ferrite magnets are most economical in fractional horsepower motors and may show an economic advantage over Alnico up to about 7.5 kW. Barium ferrite PMs are commonly used in small d.c. commutator motors for automobiles (blowers, fans, windscreen wipers, pumps, etc.) and electric toys.

Ferrites are produced by powder metallurgy. Their chemical formulation may be expressed as $\text{MO} \times 6(\text{Fe}_2\text{O}_3)$, where M is Ba, Sr, or Pb. Strontium ferrite has a higher coercive force than barium ferrite. Lead ferrite has a production disadvantage from an environmental point of view. Ferrite magnets are available in *isotropic* and *anisotropic* grades.

❖ **Rare-earth permanent magnets**

During the last three decades great progress regarding available energy density $(BH)_{max}$ has been achieved with the development of *rare-earth PMs*. The rare-earth elements are in general not rare at all, but their natural minerals are widely mixed compounds. To produce one particular rare-earth metal, several others, for which no commercial application exists, have to be refined. This limits the availability of these metals. The first generation of these new alloys based on the composition SmCo_5 and invented in the 1960s has been commercially produced since the early 1970s. Today it is a well established hard magnetic material.

SmCo_5 has the advantage of high remanent flux density, high coercive force, high energy product, linear demagnetization curve and low temperature coefficient. The temperature coefficient of B_r is 0.03 to 0.045%/°C and the temperature coefficient of H_c is 0.14 to 0.40%/°C. Maximum service temperature is 300° to 350° C. It is well suited to build motors with low volume, high power density and class of insulation F or H. The cost is the only drawback. Both Sm and Co are relatively expensive due to their supply restrictions.

With the discovery in the recent years of a second generation of rare- earth magnets on the basis of inexpensive neodymium (Nd), a remarkable progress with regard to lowering raw material costs has been achieved. This new generation of rare-earth PMs was announced by *Sumitomo Special Metals*, Japan, in 1983 at the 29th Annual Conference of Magnetism and Magnetic Materials held in Pittsburgh. The Nd is a much more abundant rare-earth element than Sm.

NdFeB magnets, which are now produced in increasing quantities have better magnetic properties than those of SmCo, but unfortunately only at room temperature. The demagnetization curves, especially the coercive force, are strongly temperature dependent. The temperature coefficient of B_r is -0.09 to $-0.15\%/^{\circ}\text{C}$ and the temperature coefficient of H_r is -0.40 to $-0.80\%/^{\circ}\text{C}$. The maximum service temperature is 250°C and Curie temperature is 350°C). The NdFeB is also susceptible to corrosion. NdFeB magnets have great potential for considerably improving the *performance-to-cost* ratio for many applications. For this reason they will have a major impact on the development and application of PM apparatus in the future.

The most important application area of rare-earth magnets with about 40% of the sales are electrical machines. Other major areas of application are actuators in data storage technology, acoustic devices, and magneto-mechanical devices (holding devices, couplings, magnetic separators, magnetic bearings). PM motors are used in a broad power range from a few mW to more than 1 MW, covering a wide variety of applications from stepping motors for wristwatches via industrial servo-drives for machine tools (up to 15 kW) to large synchronous motors. High performance rare-earth magnets have successfully replaced Alnico and ferrite magnets in all applications where the high power density, improved dynamic performance or higher efficiency are prime interest.

4.

COMSOL Multiphysics Application :-

4.1 FINITE ELEMENT METHOD AS AN AID TO MACHINE DESIGN :-

Designers of electrical machines need to satisfy the customer on a number of criteria and be competitive regarding low first and operating costs, high efficiency and reliability, minimum weight, close tolerances, etc. Moreover, new types of machines are being developed and applied. Thus it becomes increasingly essential to be able to analyse any proposed design in considerable detail, so that a near optimum may be obtained. Recent advances in Computational Electromagnetics, encouraged by continuing increase of power and speed of computers, make finite elements and related techniques an attractive alternative to well established semi-analytical and empirical design methods, as well as to the still popular 'trial and error' approach. There has been important progress in fundamental formulations providing more solid foundations for numerical field analysis.

4.2 COMMERCIAL SOFTWARE :-

A typical commercial package will have most of the following components:

Pre- and Post-Processor: fully interactive, advanced post-viewing facilities, comprehensive range of supported output devices, automatic and adaptive meshing;

Statics: magneto- and electrostatic analysis with nonlinear (and often anisotropic and hysteretic) materials, including permanent magnets, special versions for laminated materials;

Steady-state eddy currents: steady-state ac eddy current analysis, including complex permeabilities, approximate non-linear solutions

(fundamental harmonic field), background dc fields, voltage-driven problems;

Transient eddy currents: full transient analysis, nonlinear materials, multiple drives and background dc fields;

Motional eddy currents: uniform motion induced eddy-current analysis (with constant or varying topology);

Stress and thermal: mechanical stress using forces, or thermal analysis using ohmic heating, calculated from electromagnetic solutions; 2D, 2D axi-symmetric and 3D formulations.

Some of the most popular software packages:-

- COMSOL Multi Physics
- MagNet, Infolytica
- Maxwell, Ansoft
- Emag, ANSYS
- FLUX, CEDRAT Software
- MEGA, Bath University
- Integrated Engineering Software ;
- FEMM,

In our application we have used COMSOL Multi Physics.

4.3 COMSOL Multi Physics application :-

Generator in 2D---

Introduction

This example shows how the circular motion of a rotor with permanent magnets generates an induced EMF in a stator winding. The generated voltage is calculated as a function of time during the rotation. The model also shows the influence on the voltage from material parameters, rotation velocity, and number of turns in the winding.

The centre of the rotor consists of annealed medium carbon steel, which is a material with a high relative permeability. The centre is surrounded with several blocks of a permanent magnet made of samarium and cobalt, creating a strong magnetic field. The stator is made of the same permeable material as the centre of the rotor, confining the field in closed loops through the winding. The winding is wound around the stator poles. Figure 1 shows the generator with part of the stator sliced in order to show the winding and the rotor.



Figure 4.1

[Drawing of a generator showing how the rotor, stator, and stator winding are constructed. The winding is also connected between the loops, interacting to give the highest possible voltage.]

Modeling in COMSOL Multiphysics:-

The COMSOL Multiphysics model of the generator is a time-dependent 2D problem on a cross section through the generator. This is a true time-dependent model where the motion of the magnetic sources in the rotor is accounted for in the boundary condition between the stator and rotor geometries. Thus, there is no Lorentz term in the equation, resulting in the PDE

$$\sigma \frac{\partial A}{\partial t} + \nabla \times \left(\frac{1}{\mu} \nabla \times A \right) = 0$$

where the magnetic vector potential only has a z component.

Rotation is modeled using a deformed mesh application mode (ALE), in which the center part of the geometry, containing the rotor and part of the air-gap, rotates with a rotation transformation relative to the coordinate system of the stator. The rotation of the deformed mesh is defined by the transformation

$$\begin{bmatrix} x_{rot} \\ y_{rot} \end{bmatrix} = \begin{bmatrix} \cos(\omega t) & -\sin(\omega t) \\ \sin(\omega t) & \cos(\omega t) \end{bmatrix} \cdot \begin{bmatrix} x_{stat} \\ y_{stat} \end{bmatrix}$$

The rotor and the stator are drawn as two separate geometry objects, so it is possible to use an assembly (see “Using Assemblies” on page 413 of the *COMSOL Multiphysics Modeling Guide* for further details). This has several advantages: the coupling between the rotor and the stator is done automatically, the parts are meshed independently, and it allows for a discontinuity in the vector potential at the interface between the two geometry objects (called slits). The rotor problem is solved in a rotating coordinate system where the rotor is fixed (the rotor frame), whereas the stator problem is solved in a coordinate system that is fixed with respect to the stator (the stator frame). An identity pair connecting the rotating rotor frame with the fixed stator frame is created between the rotor and the stator. The identity pair enforces

continuity for the vector potential in the global fixed coordinate system (the stator frame).

The material in the stator and the center part of the rotor has a nonlinear relation between the magnetic flux, B and the magnetic field, H , the so called B-H curve. In COMSOL Multiphysics, the B-H curve is introduced as an interpolation function. The function can be used in the subdomain settings. Usually B-H curves are specified as $| B |$ versus $| H |$, but the perpendicular waves application mode must have $| H |$ versus $| B |$. It is therefore important that the H-data is entered as $f(x)$ -data of the interpolation function and the B-data entered as x -data. This relationship for $| H |$ is predefined for the material Soft Iron (without losses) in the materials library that is shipped with the AC/DC Module, `acdc_lib.txt`.

The generated voltage is computed as the line integral of the electric field, E , along the winding. Because the winding sections are not connected in the 2D geometry, a proper line integral cannot be carried out. A simple approximation is to neglect the voltage contributions from the ends of the rotor, where the winding sections connect. The voltage is then obtained by taking the average z component of the E field for each winding cross-section, multiplying it by the axial length of the rotor, and taking the sum over all winding cross sections.

$$V_i = NN \sum_{windings} \frac{L}{A} \int E_2 dA$$

where L is the length of the generator in the third dimension, NN is the number of turns in the winding, and A is the total area of the winding cross-section.

Modeling Using the Graphical User Interface--

- ❖ Model Navigator:- 2D is selected in *Space dimension* list. In *AC/DC Module* folder, *Rotating Machinery* > *Rotating Perpendicular Currents* is selected .
- ❖ Options and Settings:- From *Option* menu constants are set accordingly,

NAME	EXPRESSION	DESCRIPTION
t	0[s]	Time for stationary solution
Rpm	60[1/min]	Revolutions per minute
A	$\text{Pi} \cdot (0.02[\text{m}])^2$	Area of wires in the stator
L	0.4[m]	Length of the generator
NN	1	Number of turns in stator winding

- ❖ Geometry Modeling:- The 2D model of a generator can be imported from CAD Data Form File or can be drawn in COMSOL Multiphysics environment .(The details are not provided)

The geometry in the drawing area should now look like that in Figure 2

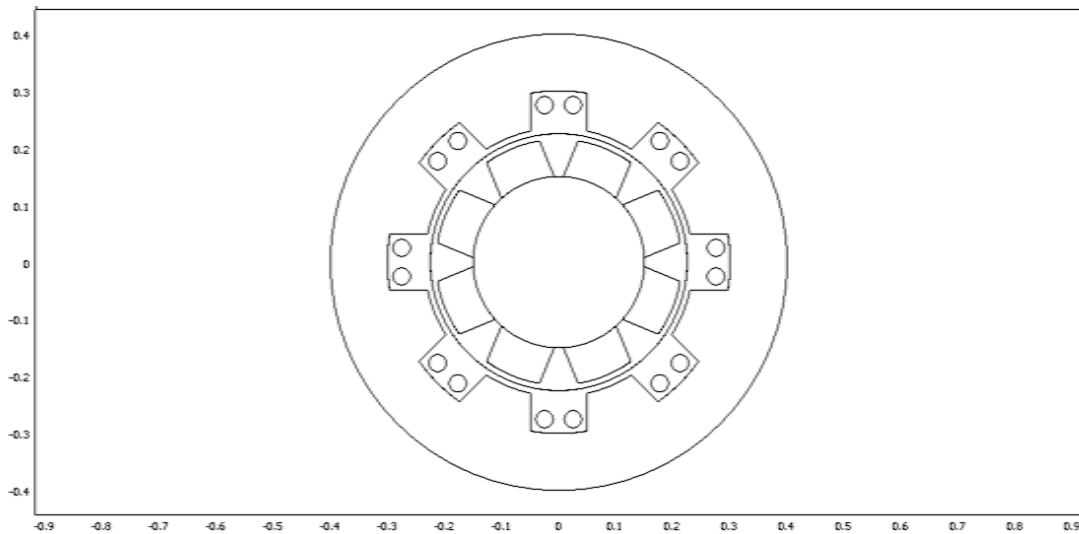




Figure 4.2

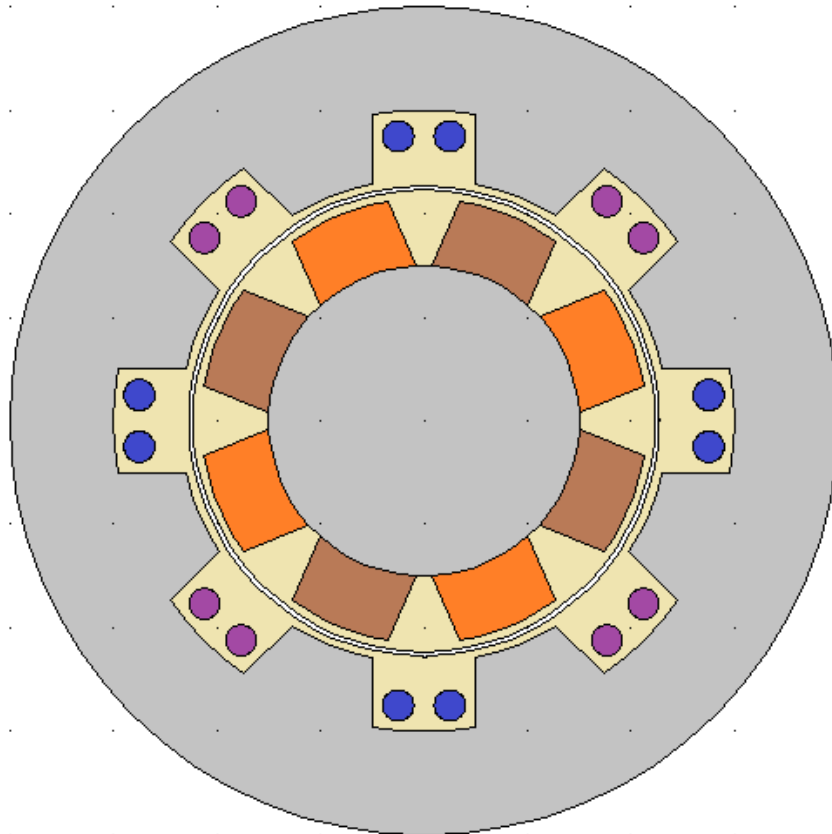
[Generator geometry]

- ❖ Assemble the Geometry:- We have now created two separate geometry objects in an assembly. We have also created an identity pair connecting the physics in the rotor and the stator, taking the rotation into account. An interface between two assemblies is actually two groups of overlapping boundaries that are, without the pair connection, completely separated in terms of mesh and solution variables. This is necessary to allow a sliding mesh at the interface between the stator and rotor where the solution variable becomes discontinuous across that interface.

Physics Settings--




- ❖ Sub-domain Variable:- From the *Option* menu point to *Integration Coupling Variables* and *Subdomain Variables* is selected.

NAME	EXPRESSION IN  COLOURED SUB- DOMAINS	EXPRESSION IN  COLOURED SUB- DOMAINS
Vi	$-L \cdot E_{z_emqa} / A$	$L \cdot E_{z_emqa} / A$



[Generator Geometry with colour coded sub-domains]

- ❖ Sub-domain settings:- sub-domain material selection

Sub-domain colours	B & H relationship	Library material
	$B = \mu_0 \mu_r H + B_r$	Samarium Cobalt (Radial, inward)
	$B = \mu_0 \mu_r H + B_r$	Samarium Cobalt (Radial, outward)
	$H = f(B)e_B$	Soft Iron
All other sub-domains	$B = \mu_0 \mu_r H$	

All the sub-domain in rotor part is rotating in counter clockwise direction.

- ❖ Boundary conditions:- the boundary settings at their defaults. The identity pair creates a coupling between the rotor and the stator in the ALE frame.
- ❖ MESH Generation:- from *MESH* menu free mesh parameters are set with specific setting.

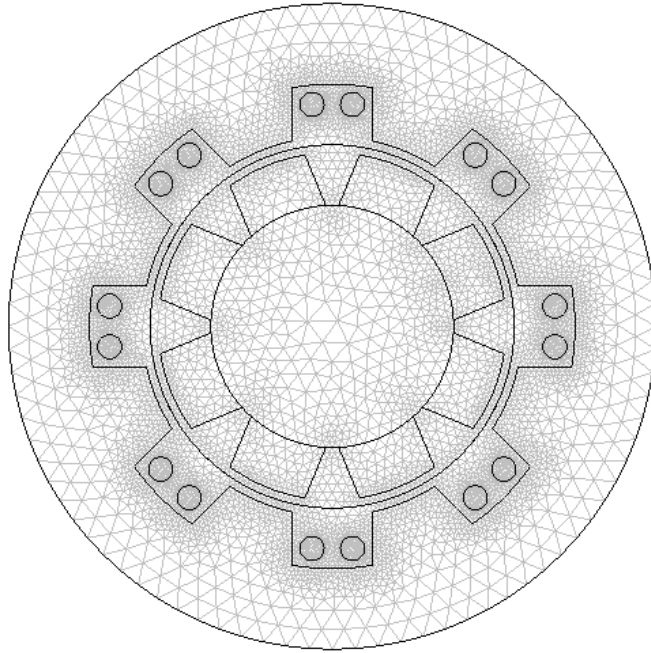


Figure 4.3
[MESH mode]

Computing the Solution--

computing the initial solution for the subsequent time-dependent simulation for both static and transient analysis.

Static Analysis :-

In *Solver Parameters* dialog box *Auto select Solver* is selected and *Static* from *Analysis list* is also selected.

Simulation of the generator with the rotor in motion. By default, the calculated solution will be used as the initial solution.

Transient Analysis :-

In *Solver Parameter* dialog box *Transient* from the *Analysis list* is selected. In the *Times* edit field (*Time stepping*) input is given as followed-

Time: linspace(0, 0.25 ,26)

Relative Tolerance: 1e-2

Absolute Tolerance: Az 1e-3 lm1 5e3

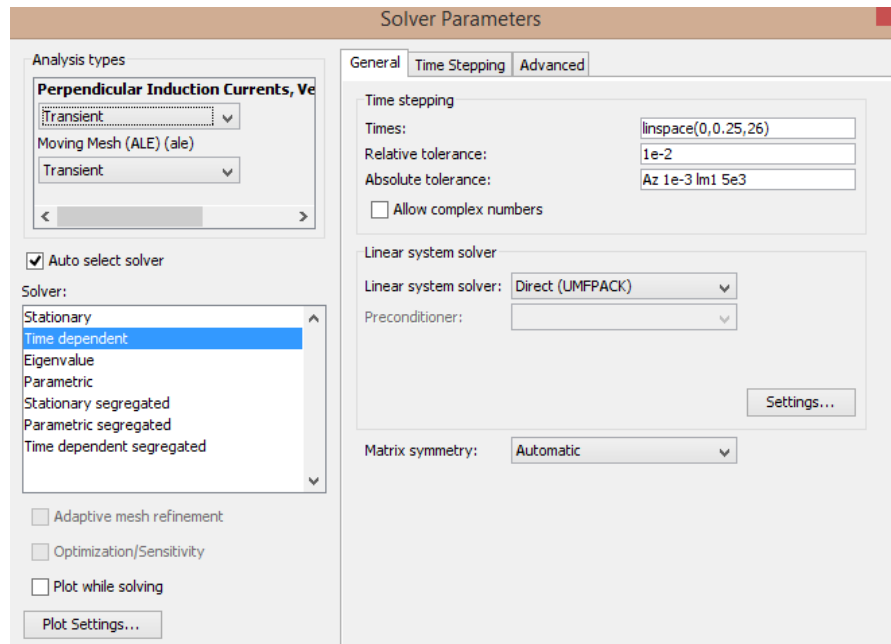


Figure 4.4

[Solver Parameter setting during Transient Analysis]

After selecting the solve menu,

Output : Flux density spectrum-

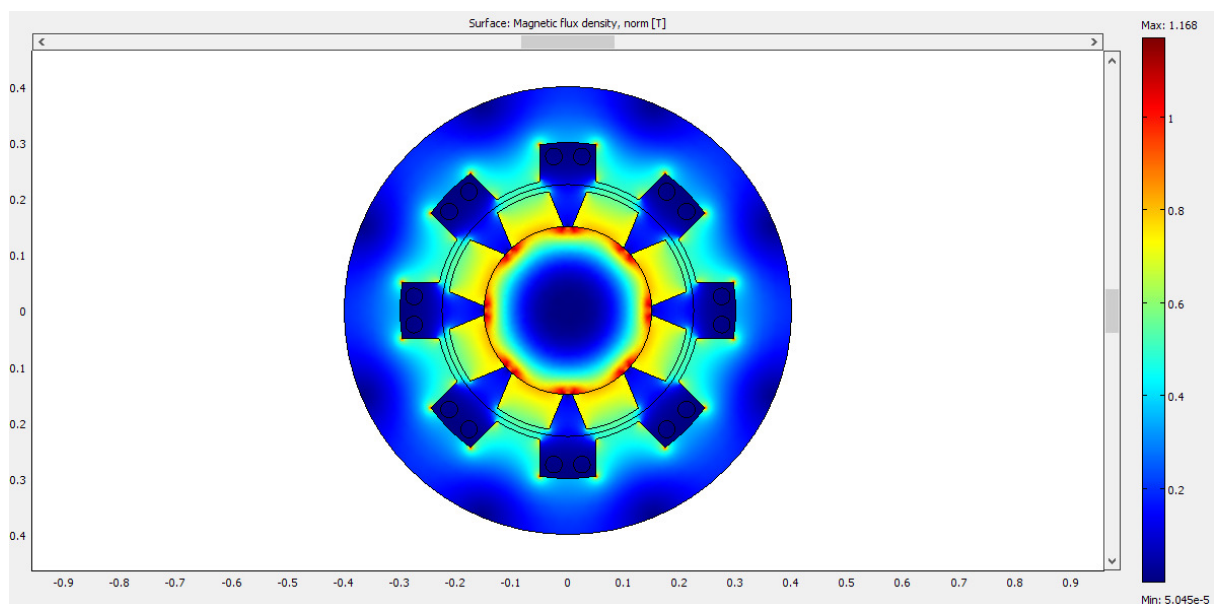


Figure 4.5

[Magnetic flux density spectrum]

Post-processing and Visualization--

From the *Postprocessing* menu *Plot Parameters* dialog box is opened and the setting is made accordingly,

On *General* page, *Solution at time* list is selected 0.2 sec.

On *Surface* page, *Predefined Quantities* list *Magnetic flux Density, norm* is selected.

On *Contour* page, *Levels* is given 15 and *Contour Plot* is selected.

On *Boundary* page *Boundary Plot* is selected.

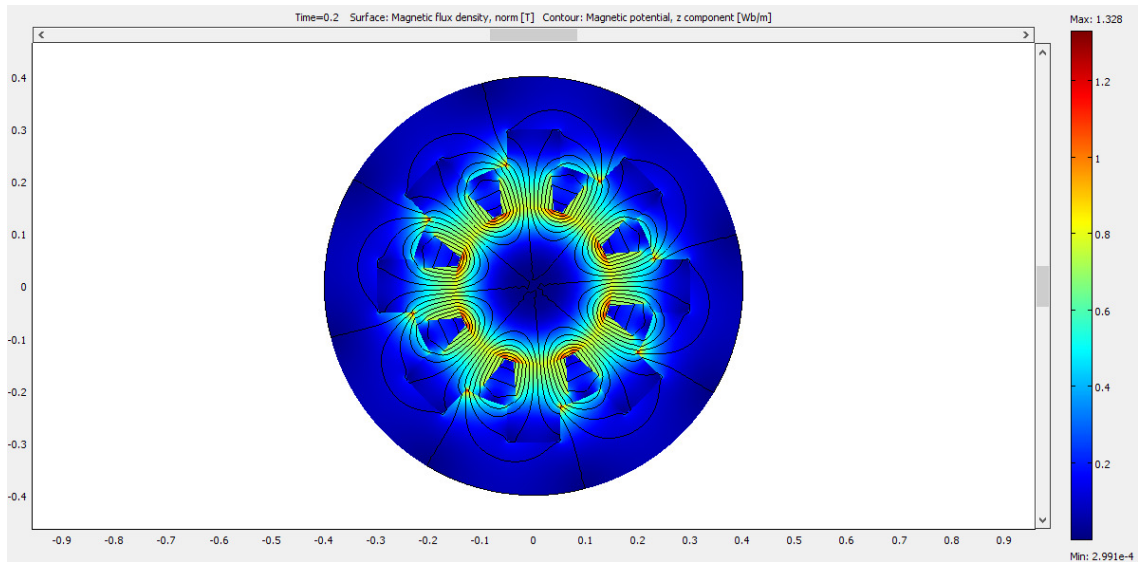


Figure 4.6

[Magnetic flux density spectrum with contour]

To view the induce voltage as a function of time,

From the *Postprocessing* menu *Domain Plot Parameters* is selected,

On *Point* page *Expression* is given $V_i * NN$.

Results and Discussion:-

- **Condition 1** : rpm-60 , Number of turns in Stator winding-1 , Permanent Magnet used in rotor- Smarium Cobalt.

The generated voltage in the rotor winding is a sinusoidal signal. At a rotation speed of 60 rpm the voltage will have an amplitude around 2.3-2.5 V for a single turn winding.

Voltage output-

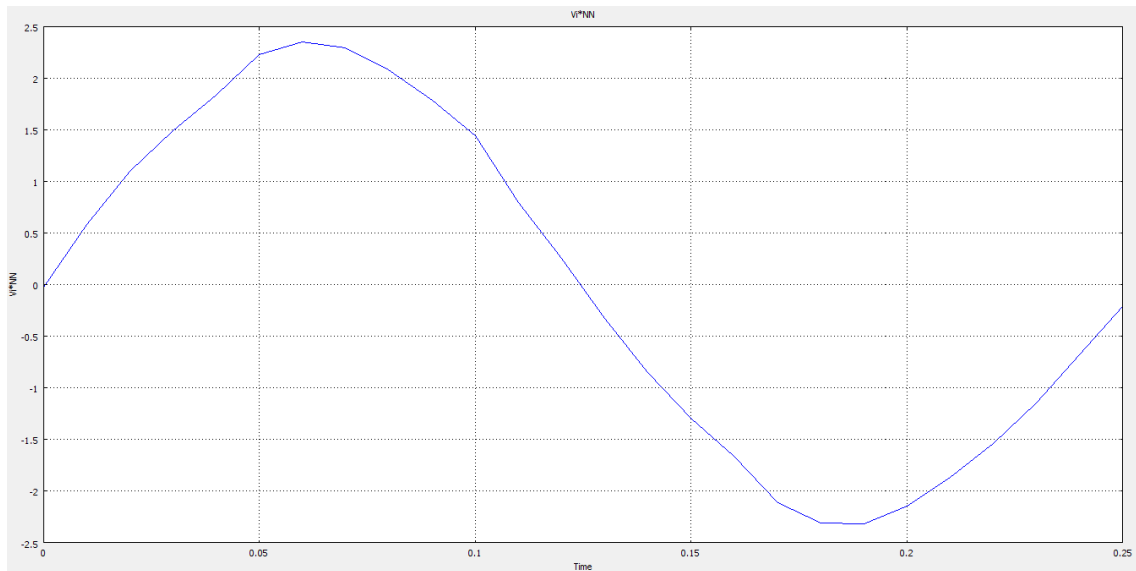


Figure 4.7

[The generated voltage over one quarter of a revolution. This simulation used a single-turn winding.]

- **Condition 2 : rpm- 750, Number of turns in Stator winding-1 ,**
Permanent Magnet used in rotor- Smarium Cobalt.

The generated voltage in the rotor winding is a sinusoidal signal. At a rotation speed of 750 rpm the voltage will have an amplitude around 28 -30 V for a single turn winding.

Voltage output-

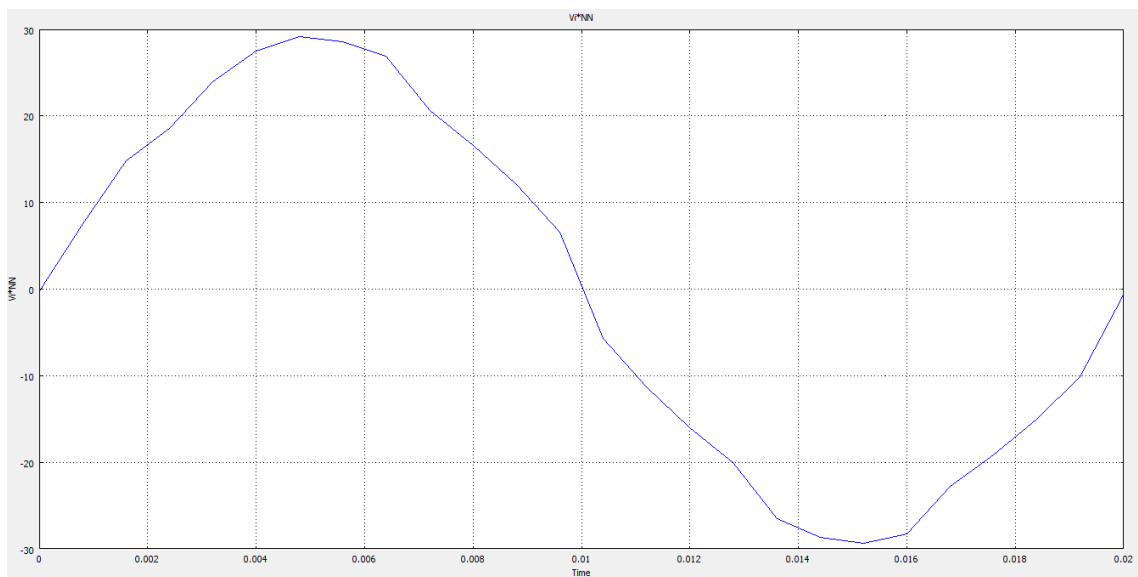


Figure 4.8

[The generated voltage over one quarter of a revolution. This simulation used a single-turn winding.]

- **Condition 3 : rpm- 750, Number of turns in Stator winding-5 , Permanent Magnet used in rotor- Smarium Cobalt.**

The generated voltage in the rotor winding is a sinusoidal signal. At a rotation speed of 750 rpm the voltage will have an amplitude around 140-150 V for five turns winding.

Voltage output-

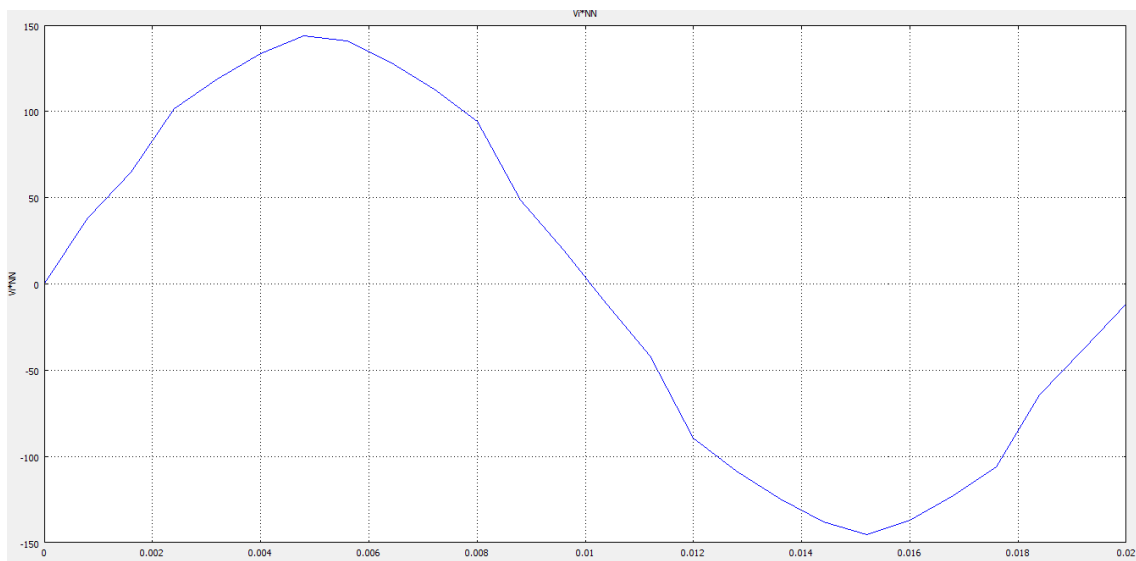


Figure 4.9

[The generated voltage over one quarter of a revolution. This simulation used a five turns winding.]

So, it is clear that with increasing the revolution per minute , the generated voltage is increasing and also with increasing the turn of stator winding, the generated voltage is increasing proportionally.

Conclusion

All electrical Machine converts electrical energy to mechanical energy or mechanical energy to electrical energy. The calculation of magnetic fields in electrical machine with the aid of Finite Element Analysis Method enables a more accurate calculation of characteristics and parameters of electrical machine. However Finite Element Analysis Method call for retaining a no of assumptions , the legitimacy of which are not always un-quittance. However the inclusion of this and to calculate magnetic high by FEM computer consumes so high time, so that it becomes impracticable. We have assumed 2D model by symmetry of the machine, but in case of 3D model it takes a special long time and large memory size. So the computer system should be upgraded for the 3D model.

Due to efforts of various scientists it has become possible to evaluate the calculation method based on the representation of the field of real winding as a set of high of simplest loop, disposed on care. The FEM developed so far displays exceptional flexibilities in breaking down the space electromagnetic field destined of calculation. The calculation of EM field in electrical machine which have boundaries complex in configuration and exhibit non-linearity and induced current will be scope of future work.

The standard design calculation for a machine based on lump parameter and flux distribution which exhibits the flux internal distribution of a machine is non-realistic but FEM results on the analyzed machine depicts the actual distribution of flux at the various important point of the machine across the cross section. Using this distribution of flux along the air-gap up-to 360° , one can calculate the electro-magnetic energy into the air-gap , electro-magnetic force and torque developed into the machine. Due to limitation of time the above study could be a future work.

REFERENCES

- Juha Pyrhönen , Tapani Jokinen and Valéria Hrabovcová ; "Design of Rotating Electrical Machines " ; John Wiley & Sons, Ltd., 2008.
- B. Schwarz ; "Geometrical approach to the economical design of rotating electrical machines" ; IET Journals & Magazines, 1966.
- Matthew N. O. Sadiku ; "Elements of Electromagnetics" ; The Finite Element Method part.
- P. P. Silvester and R. L. Ferrari ; " Finite Elements for Electrical Engineers" ; Cambridge, England: Cambridge Univ. Press, 1983.
- Jacek F. Gieras, Mitcheli Wing ; "Permanent Magnet Motor Technology- Design and Application" ; Permanent Magnet Materials part.
- A. E. Fitzgerald , Charles Kingsley, Jr., Stephen D. Umans ; "Electric Machinery " ; Properties of Magnetic Materials part.
- Charanjiv Gupta, Sanjay Marwaha and Manpreet Singh Manna ; "Finite Element Method as an aid to Machine Design : A Computational Tool" ; COMSOL Conference 2009 Bangalore.
- AC/DC Module - Model Library ; COMSOL Multiphysics user guide.